Proceedings of the 2009 IEEE International Conference on Systems, Man, and Cybernetics
San Antonio, TX, USA - October 2009

Trans-skull Imaging System by Ultrasonic Array Probe

Genta Hiramatsu, Yuichiro Ikeda, Syoji Kobashi, Yutaka Hata
Graduate School of Engineering, University of Hyogo
2167, Shosha, Himeji, Hyogo, 671-2280, Japan
hata@ieee.org

Seturo Imawaki
Ishikawa Hospital
2-150 Bessho, Bessho-cho, Himeji, 671-0221, Japan

Yuri Kitamura, Toshio Yanagida
Graduate School of Frontier Biosciences, Osaka University
1-3, Yamadaoka, Suita, Osaka, 565-0871 Japan

***Abstract* —In this paper, we propose a trans-skull imaging system of the human brain using an ultrasonic array probe. In it, we employ a cow scapula imitated to human skull and a steel with ditches imitated to cerebral sulci. We scan the phantom consisting of the bone and steel ditches by a 32channel array probe and obtain the B-mode image. From the B-mode image, we extracted the bone thickness by fuzzy inference, and visualize the ditches by filtering techniques. Experimental result shows that the mean error of bone thickness is less than 1mm and that the mean errors of the ditch width and depth are 6.9mm and 2.8mm, respectively.**

***Keywords*— ultrasonic system, fuzzy inference, thickness determination, brain imaging**

I. INTRODUCTION

The imaging of the human brain is essential to diagnose the brain. Currently, X-ray computed tomography (CT) and magnetic resonance imaging (MRI) are widely used. These systems can obtain the detailed image of the brain. However, these systems are not real-time imaging system. In addition, X-ray CT has a serious problem of X-ray exposure. Therefore, the noninvasive and real-time imaging system is required.

As the noninvasive system, the ultrasonic device is widely used [1], [2]. The ultrasonic devices have some advantages such as real-time imaging system and low cost and small in comparison with MRI and the X-ray CT. In the clinical practice, the ultrasonic devices with the center frequency of 2-10 MHz are used to visualize internal organs in the human body [3]. However, ultrasound attenuates by absorption and dispersion when the ultrasound transmits and receives the object. In particular, the ultrasound attenuates when the ultrasound transmits and receives the hard tissue such as the bone, so it becomes difficult to receive the echo. Therefore, the clinical practice of trans-bone is not done except for diagnosing osteoporosis. However, it is known that the low frequency ultrasound approximately 1MHz can transmit and receive the bone tissue. Therefore, the study intended the bone is performed actively with the low frequency ultrasound [4-6]. In Reference [4], transcranial sonography has been proposed using two linear array probes. This array probe consists of 128 elements. However, it is difficult to transmit ultrasound from the random position because the two array probes are set up on both sides of human brain. In References [5] and [6], imaging system of the skull and brain surface has been proposed using a single ultrasonic probe whose center frequency is 1.0 MHz. In this system, a target object is scanned with 1.0 mm scanning interval using a 3-D scanner. So, it is difficult to apply it to clinical practice because this scanner is too large to use clinical practice. Then, the human body is constrained. A simple and unrestrained system without the large mechanical scanner is required.

In this study, we employ a 32channel array probe with the center frequency of 1MHz by manual operation and perform imaging of the sulcus surface. The array probe is a device which can obtain plural data at once. We propose a fuzzy imaging system for human brain by the ultrasonic array probe. We employ a cow scapula imitated to human skull and a steel with ditches imitated to cerebral sulci. First, we scan the phantom consisting of the bone and steel ditches by the 32channel array probe and obtain the B-mode image. Then, we extract the skull surface echo. Second, we determine the bottom of the skull by a fuzzy inference [7], [8]. Then, we calculate the skull thickness between the surface and bottom points. Finally, we extract the ditches shape of the object. In our experiment, we visualized the cow scapula thickness with high accuracy. The ditches of the steel were also visualized clearly.

II. ULTRASONIC ARRAY PROBE

Fig. 1 shows the system of our newly developed ultrasonic array probe (ISL Inc., ISL1938). The array probe consists of 32 elements and the elements are in a line with 1.5 mm interval. The center frequency of the elements is 1.0MHz. As shown in Fig. 2 (a), the voltage is applied to adjacent several elements. We can arbitrarily set the number of elements applying the voltage and the number called simultaneous activating number. The ultrasounds are generated from each element. The combination of ultrasounds is generated by synthesizing the ultrasounds. Moreover, the applied voltage shifts by 1 element distance. The array probe can continuously generate the combination of ultrasound by repeating the shift of applied voltage. In Fig. 2, the simultaneous activating number is 3, and

978-1-4244-2794-9/09/$25.00 ©2009 IEEE

the array probe can generate 30 combinations of ultrasounds. Moreover, the obtained amount of data is equivalent to the amount of data scanned for 45mm by the single probe. The distance between the elements is 1.5mm.

A. *Experimantal materials*

In this study, we employ a cow scapula imitated to human skull and a steel with ditches imitated to cerebral sulci. We scan the phantom consisting of the bone and steel ditches by a 32channel array probe and obtain the B-mode image. Fig. 3 shows the cow scapula. The cow scapula has the thickness from 4.0 to 6.0 mm and has the width of 190.0 mm. In this experiment, we employ about 5.0 mm depth part of the cow scapula. Figure 4 shows the steel ditch. Table I show the specification of the steel ditch. Fig. 5 shows the ultrasonic data acquisition system. The water temperature is kept with 20 degrees by a thermostat water bath (Thomas Kagaku Co. Ltd., T-22L). The cow scapula and the steel ditch are put in the thermostat water bath. In this experiment, we obtain the ultrasonic data by manually scanning using the array probe. The ultrasonic flaw detector (Eishin Kagaku Co. Ltd., MC-64) transmits and receives ultrasound via the array probe. The sampling interval is 20 ns.

III. OUR PROPOSED METHOD

This section describes an imaging method for ditches imitated as cerebral sulcus using the ultrasonic array probe. First, we extract the bone surface echo. We calculate the correlation coefficient between the bone surface echo and the every waveform to decide the surface point. Second, we determine the bottom point of the bone by using a fuzzy inference. Then, we calculate the bone thickness between the surface point and the bottom point. Finally, we extract the surface shape of the steel ditch under the bone by filtering techniques. The details of this process are as follows.

A. *Calculation of Bone Thickness*

It is necessary to determine the surface point and the bottom point of the bone to calculate the thickness. First, we determine the surface point of the bone. The reflection echo from the bone surface is first received. To determine the surface point, we calculate the correlation coefficient between the extracted surface echo and every waveform. The correlation coefficient r is calculated by Equation (1).

$$r = \frac{\frac{1}{n-1}\sum_{i=1}^{n}\left(X_i - \overline{X}\right)\left(Y - \overline{Y}\right)}{\sqrt{\frac{1}{n-1}\sum_{i=1}^{n}\left(X - \overline{X}\right)^2}\sqrt{\frac{1}{n-1}\sum_{i=1}^{n}\left(Y - \overline{Y}\right)^2}} \tag{1}$$

In Equation (1), the notation X denotes the surface echo data, the notation $\overline{X}$ denotes the average of surface echo data, the notation Y denotes the acquisition waveform data, and the notation $\overline{Y}$ denotes the average of the acquisition waveform data. We determine the point with the highest correlation coefficient as the surface point of the bone.

Next, we determine the bottom point of the bone. In this study, we determine the bottom echo point using fuzzy

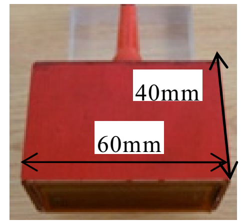

Figure.1. Our newly developed ultrasonic array probe

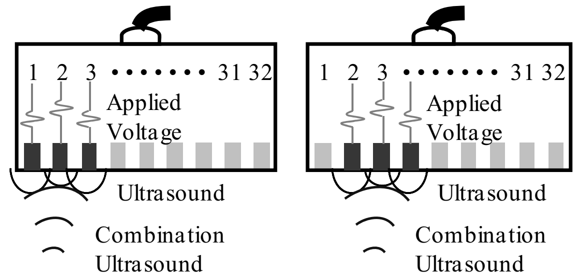

(a) Combination ultrasound (b) Electronic control shift
Figure.2. The system of our array probe

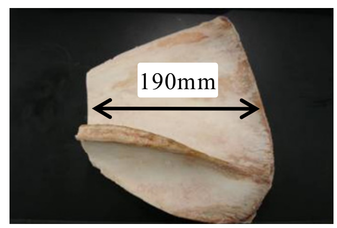

Figure.3. The cow scapula

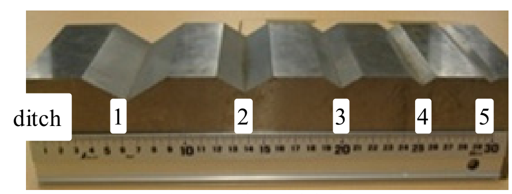

Figure 4. The steel ditch

TABLE I
THE SPECIFICATION OF THE STEEL WITH DITCH

	Ditch1	Ditch2	Ditch3	Ditch4	Ditch5
width[mm]	51.96	34.64	24.25	17.32	10.39
depth[mm]	15.00	10.00	7.00	5.00	3.00

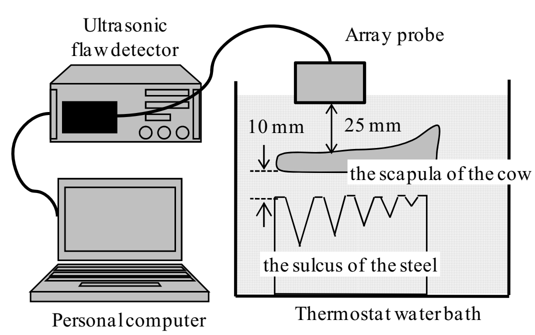

Figure.5. Ultrasonic data acquisition system.

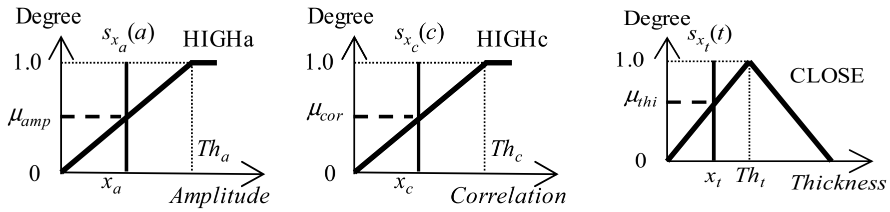

(a) Amplitude (b) Correlation (c) Thickness

Figure.6. Fuzzy membership function

inference. The ultrasound reflects at the boundary between water and the bone because the cow scapula acoustic impedance is quite different from the water acoustic impedance. Therefore, the amplitude of reflection echo enlarges in proportion to the difference of the acoustic impedance. The phase and frequency of the bottom echo and the surface echo are approximately similar because these echoes are part of the ultrasonic transmission echo. Therefore, the correlation coefficient between the bottom echo and the surface echo is high. Moreover, the distance between the surface echo and the bottom echo is proportional to the thickness of the bone. From these facts, we can obtain three knowledge as follows.

Knowledge 1: The amplitude of the bottom echo of the bone is large.

Knowledge 2: The correlation coefficient between the surface echo and the bottom echo of the bone is high.

Knowledge 3: Interval distance between the surface and the bottom echoes depends on the thickness.

The following fuzzy if-then rules are derived from three knowledge.

Rule 1: IF *Amplitude* is *High* THEN the degree of bottom is High.

Rule 2: IF *Correlation* is *High* THEN the degree of bottom is High.

Rule 3: IF *Thickness* is *Close* to the assumed thickness THEN the degree of bottom is High.

The fuzzy if-then rules are represented by the fuzzy membership functions as shown in Fig. 6. In Fig. 6, The notations, Th_a, Th_c and Th_t denote thresholds of *Amplitude*, *Correlation* and *Thickness*, respectively. The Th_a is determined as the maximum of the amplitude of the acquisition waveform. The Th_c is determined as 1.0. The Th_t is the assumed thickness. Three fuzzy degrees μ_{amp}, μ_{cor} and μ_{thi} are calculated by Equations (2), (3) and (4), respectively.

$$\mu_{amp}(x) = \min\left(s_{x_a}(a),\ HIGHa\right) \tag{2}$$

$$\mu_{cor}(x) = \min\left(s_{x_c}(c),\ HIGHc\right) \tag{3}$$

$$\mu_{thi}(x) = \min(s_{x_t}(t), CLOSE) \tag{4}$$

In this method, we calculate μ_{thi} for every case of Th_t whose values take from 3.0mm to 5.0mm at the interval of 0.2mm. The fuzzy singleton functions $S_{x_a}(a)$, $S_{x_c}(c)$ and $S_{x_t}(t)$ are defined by Equations (5), (6) and (7), respectively.

$$S_{x_a}(a) = \begin{cases} 1 & \text{if } a = x_a \\ 0 & \text{otherwise} \end{cases} \tag{5}$$

$$S_{x_c}(c) = \begin{cases} 1 & \text{if } c = x_c \\ 0 & \text{otherwise} \end{cases} \tag{6}$$

$$S_{x_t}(t) = \begin{cases} 1 & \text{if } t = x_t \\ 0 & \text{otherwise} \end{cases} \tag{7}$$

The total degree μ_{bottom} is calculated by Equation (8).

$$\mu_{bottom} = \mu_{amp}(x)\times\mu_{cor}(x)\times\mu_{thi}(x) \tag{8}$$

The $\mu_{bottom}(x)$ denotes the fuzzy degree of the obstacle bottom of the bone. The point with the highest degree is determined as the bottom point. The bone thickness is calculated by the surface and the bottom points by Equation (9).

$$Thickness = \frac{1}{2}\times(t_b - t_s)\times v_m \tag{9}$$

The notations, t_b and t_s denote the bottom and the surface points, respectively. The notation v_m denotes the velocity of the bone. In this study, the velocity of the bone is 4000(m/s).

B. *Extraction of the Ditches*

We extract the ditches from the obtained gray scale image(B-mode image). Fig. 7 shows the flowchart of the extraction method of the steel with ditches. The B-mode image is derived by converting the amplitude of acquisition waveforms into gray scale intensities from 0 to 255. Fig. 8 shows the example of a B-mode image. As shown in Fig. 7 it is difficult to extract the ditch because the ditch part is low intensity. First, we apply the contrast enhancement to the B-mode image to increase the part of low intensity. The tone curve between the input and output of the intensity is shown in Fig. 9. In Fig. 9, we manually determine the threshold *Th*. Second, we apply the Median Filter to remove the noise. Third, we apply the Sharpening Filter to emphasize the change of the intensity because the ditch outline is indistinct after removing the noise. After applying the Sharpening Filter, we apply an Edge Extraction Filter to the image to extract the edge of the ditches. As shown in Fig. 10, the operator of the Edge Extraction Filter is rotated. Every rotated operator is applied to the image. In this method, we employ the 5×5 spatial filter. We rotate the filter with every 5 degree from 0 to 360, and we apply it to the image. We determine the filter coefficients using Gauss function. As shown in Fig. 11 (a), we employ the Gauss function; the mean average is 0 and the number of points is 500. We can manually determine the magnitude and standard

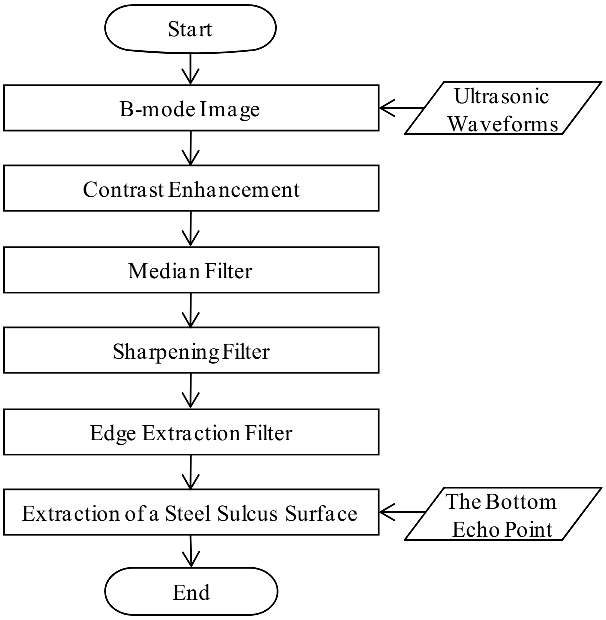

Figure.7. Flowchart of extraction method of the steel sulcus surface

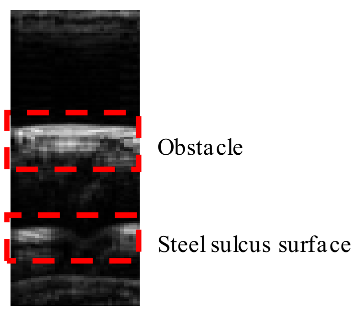

Figure.8. Example of B-mode image

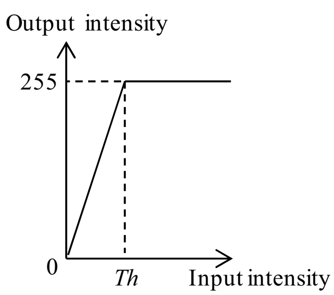

Figure.9. The input-output relation of the intensity

deviation. We derive the first-derivation Gauss function by differentiating the Gauss function as shown in Fig.11 (b). As shown in Fig. 12, the operator of the edge extraction filter is represented with 500×500 matrix using the first-derivation Gauss functions. The Gauss function $f_x(x, y)$ by differentiating x-partially is represented by Equations (10).

$$f_x = \left\{ \frac{-5.544 \times mag \times (x-250)}{\sigma^2} \right\} \times \exp\left\{ \frac{-2.772 \times (x-250)^2}{\sigma^2} \right\} \quad (10)$$

The notation mag denotes the magnitude of gauss function. The notation σ denotes the standard deviation. The obtained

Operator

0 deg

0	0	0	0	0
0.2	1.6	0	-1.6	-0.2
0.3	3.3	0	-3.3	-0.3
0.2	1.6	0	-1.6	-0.2
0	0	0	0	0

⇩ Rotation

30 deg

0	0.1	0	0	0
0.2	1.9	2.3	-0.4	0
0.3	3.6	0	-3.6	-0.4
0	0.4	-2.2	-1.9	-0.1
0	0	0	-0.1	0

⇩ Rotation

45 deg

0	0.2	0.1	0	0
0.2	1.7	3.2	0	0
0.1	3.2	0	-3.2	-0.1
0	0	-3.2	-1.8	-0.2
0	0	-0.1	-0.2	0

⇩ Rotation

⋮

Figur.10. Operator of Edge Extraction Filter

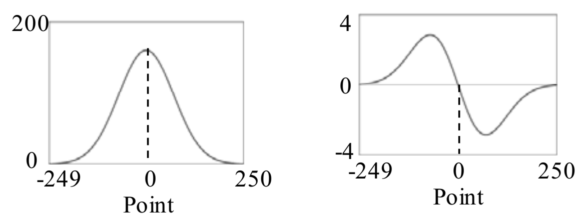

(a) Graph of gauss function (b) First derivation

Figure 11. Gauss Function

500×500 matrix is scaled down to 5×5 matrix. When we apply the Edge Extraction Filter, we calculate the intensities by Equations (11).

$$Out_{\langle angle \rangle}(x, y) = \sum_i \sum_j operator(i, j) \times In(x+i, y+j) \quad (11)$$

The notation *operator* denotes the operator of the Edge Extraction Filter. The notation *In* denotes the the image.

We determine the maximum intensity of the each angle as the output intensity for the interest pixel. We apply this process to all pixels of the image. Thus, we image the ditches from the extracted edge image. Next, we derive a binary image of the ditches. Fig. 13 shows the extraction algorithm for obtaining the binary image. First, we determine the initial search point below. In left edge pixel with high intensity of the extracted edge image, we perform the raster scanning to search the pixel whose intensity is larger than the threshold, and we determine the first detected pixel as the initial point of the ditches. Second, we move the interest pixel from the determined surface point to 1 pixel right. We determine this moved interest pixel as new interest pixel. We search the neighboring 5 pixels from the new one. In the searching pixels, we determine the point which the maximum intensity as the ditch pixel. This process is repeated until the interest pixel is reached to right edge of the image.

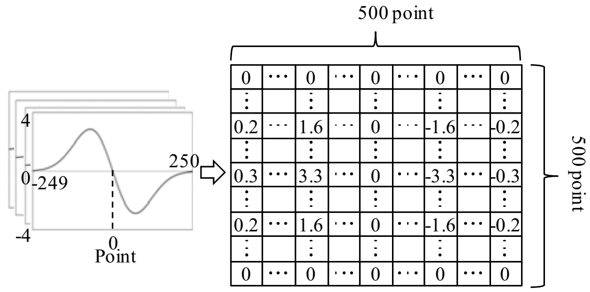

Figur.12. Derivation of Operator of Edge Extraction Filter

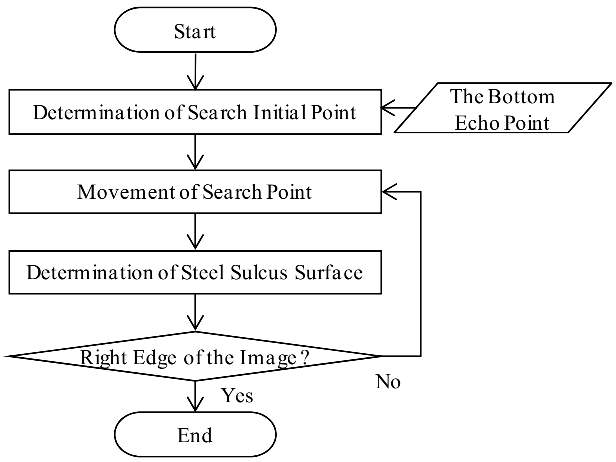

Figur.13. Extraction algorithm of the steel sulcus surface

IV. Experimental Result

We applied our proposed method to the brain model with the cow scapula and the steel ditch. We set the array probe as shown in Fig. 5, where we set the simultaneous activating number to 1. We obtained the ultrasonic waveforms from every ditch. First, we applied our proposed method to an obtained ultrasonic waveform and calculated the cow scapula thickness. Table II shows the measurement result of the cow scapula thickness. As shown in Table II, we calculated the cow scapula thickness from 4.40 mm to 5.32 mm. We thus calculated the cow scapula thickness with the high accuracy. Here, the cow scapula used in this experiment has the thickness from 4.0 mm to 6.0 mm. Second, we image the ditches of the steel as the model of cerebral sulci. Fig. 14 shows the extracted images. Thus, we extracted the ditch parts. Table III and IV show the results of the ditch widths and depths, respectively. As shown in Table III, the ditch widths were extracted within the mean error of 6.9 mm. Moreover, as shown in Table IV, the ditch depths were extracted within the mean error of 2.8 mm.

V. Conclusion

In this paper, we have proposed a fuzzy imaging system for human brain by an ultrasonic array probe. By using the array probe, the ultrasonic waveform was easily obtained without mechanical scanning of the ultrasonic probe. In this method, we did the experiment using the cow scapula as human skull and the ditches of the steel as human cerebral sulci. From the obtained ultrasonic data, we calculate the bone thickness using fuzzy inference. Next, we extract the ditches from the B-mode image. As the result, we calculated the cow scapula thickness with high accuracy. Moreover, we extracted the ditches from the B-mode image and calculated the ditch width within the mean error less than 6.9mm and the depth within the mean error less than 2.8mm. Therefore, we showed the effectiveness of our proposed method.

TABLE II
MEASUREMENT RESULT OF THE COW SCAPULA THICKNESS

	Thickness (mm)		Thickness (mm)
ch1	4.92	ch17	5.20
ch2	4.80	ch18	5.32
ch3	4.56	ch19	5.24
ch4	4.76	ch20	4.68
ch5	4.96	ch21	4.60
ch6	5.00	ch22	5.12
ch7	4.96	ch23	4.64
ch8	4.56	ch24	5.12
ch9	4.52	ch25	5.12
ch10	4.52	ch26	5.08
ch11	4.64	ch27	5.04
ch12	4.68	ch28	5.00
ch13	5.12	ch29	4.40
ch14	4.64	ch30	4.52
ch15	4.64	ch31	4.48
ch16	4.60	ch32	4.96

Acknowledgment

This work was supported in part by Japan Society for the Promotion of Science with Grant-in-Aid for Scientific Research (B) (KAKENHI 20390329).

References

[1] K. A. Wear, “Autocorrelation and Cepstral Methods for Measurement of Tibial Cortical Thickness,” IEEE Transactions on Ultrasonics, Ferroelectrics, and Frequency Control, Vol.50, No.5, pp.655-660, June 2003.

[2] J. Krautkramer and H. Krautkramer, ed., “Ultrasonic Testing of Materials,” Springer-Verlag, 1990.

[3] Thomas R. Nelson, etc, Three-Dimensional Ultrasound, Lippincott Williams & Wilkins, 1999.

[4] F. Vignon, J. -F. Aubry, M. Tanter, A. Margoum, and M. Fink, “Dual-Arrays Brain Imaging Prototype: Experimental In Vitro Results,” IEEE International Ultrasonics Symposium, pp. 504-507, 2005.

[5] Y. Hata, S. Kobashi, K. Kondo, Y. T. Kitamura, and T. Yanagida, “Transcranial Ultrasonography System for Visualizing Skull and Brain Surface Aided by Fuzzy Expert System,” IEEE Trans. on Systems, Man and Cybernetics, pp. 1360-1373, Vol. 35, No. 6, 2005.

[6] M. Kimura, S. Kobashi, K. Kondo, Y. Hata, Y. T. Kitamura, and T. Yanagida, "Fuzzy Ultrasonic Imaging System for Visualizing Brain Surface under Skull Considering Ultrasonic Refraction," in Proc. 2006 IEEE International Conference on Systems, Man, and Cybernetics, pp. 3790-3794, 2007.

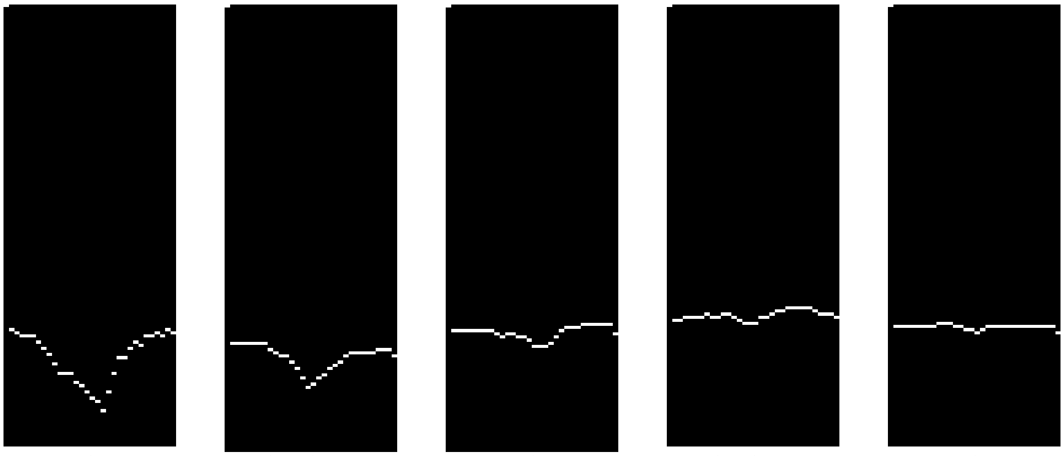

(a) Sulcus 1. (b) Sulcus 2. (c) Sulcus 3. (d) Sulcus 4. (e) Sulcus 5.

Figure.14. Extraction Results of Steel Sulcus Surface

TABLE III
MEASUREMENT RESULT OF THE STEEL SULCUS WIDTHS

	Sulcus 1	Sulcus 2	Sulcus 3	Sulcus 4	Sulcus 5
Measurement value [mm]	45.0	31.5	22.5	16.5	9
True value [mm]	51.9	34.6	24.2	17.3	10.3
Absolute error [mm]	6.9	3.1	1.7	0.8	1.3

TABLE IV
MEASUREMENT RESULT OF THE STEEL SULCUS DEPTHS

	Sulcus 1	Sulcus 2	Sulcus 3	Sulcus 4	Sulcus 5
Measurement value [mm]	15.6	9.0	4.2	3.0	2.4
True value [mm]	15.0	10.0	7.0	5.0	3.0
Absolute error [mm]	0.6	1.0	2.8	2.0	0.6

[7] J. Yasui, S. Kobashi, K. Kondo and Y. Hata, "Fuzzy Ultrasonic Testing System with Columnar Rod," Proc. of 2006 International Symposium on Intelligent Signal Processing and Communication Systems (ISPACS 2006), pp. 903-906, Dec. 2006.

[8] L. A. Zadeh and J. Kacprzyk, Fuzzy Logic for the Management of Uncertainly. New York: Wiley, 1992.